Supporting information

Controlling DOSC of Surface Faradaic Layers on Fe_2O_3 Photoanodes for Solar Rechargeable Devices

Dongjian Jiang[1], Xiao Sun[1], Mengfan Xue[2], Pin Wang[2], Yingfang Yao[1], Wenjun Luo[1]*, Zhigang Zou[1,2]

[1]National Laboratory of Solid State Microstructures, College of Engineering and Applied Sciences, Nanjing University, Nanjing 210093, China

[2]Eco-materials and Renewable Energy Research Center (ERERC), Jiangsu Key Laboratory for Nano Technology, National Laboratory of Solid State Microstructures and Department of Physics, Nanjing University, Nanjing 210093, China

*Email: wjluo@nju.edu.cn;

Experimental section

Preparation of Fe_2O_3 and Ti-Fe_2O_3 photoanodes

The Fe_2O_3 and Ti-Fe_2O_3 photoanodes were prepared by hydrothermal methods[1]. 0.15 M $FeCl_3$ and 1 M $NaNO_3$ were dissolved in 100 mL deionized water as precursor solution, and then the solution was delivered into a 50 mL Teflon-lined stainless steel autoclave. A hydrothermal reaction was carried out at 100 °C for 1 hour. Subsequently, the obtained FeOOH was annealed at 800 °C for 5 min to obtain a Fe_2O_3 film. A Ti-Fe_2O_3 film was also prepared using the similar procedure except the addition of 100 μL $TiCl_3$ solution into the precursor solution before the hydrothermal reaction.

Preparation of $Fe_2O_3/NiCoO_xH_y$, Ti-$Fe_2O_3/NiCoO_xH_y$ and FTO/$NiCoO_xH_y$ electrodes

The $NiCoO_xH_y$ was prepared on FTO, Fe_2O_3 and Ti-Fe_2O_3 by electrodeposition[2], respectively. The $Co(NO_3)_2{\cdot}6H_2O$ and $Ni(NO_3)_2{\cdot}6H_2O$ with molar ratio of Co^{2+} and Ni^{2+} as 1:1 were dissolved in the deionized water. Then the $NiCoO_xH_y$ samples were deposited onto different substrates at -0.5 mA/cm^{-2} for 10 s in a three-electrode-cell, with a platinum wire counter electrode and the saturated calomel electrode (SCE) as a reference electrode.

Construction of solar rechargeable devices

Solar rechargeable devices were assembled by connecting $Fe_2O_3/NiCoO_xH_y$ and Ti-$Fe_2O_3/NiCoO_xH_y$ photoanodes with carbon cloth (Taiwan Carbon Energy Technology, W0S1002) counter electrodes, which were labeled as $Fe_2O_3/NiCoO_xH_y/KOH_{(aq)}$/carbon and $Fe_2O_3/NiCoO_xH_y/KOH_{(aq)}$/carbon, respectively. The electrolytes were 1 M KOH (pH = 13.6) aqueous solution.

Morphological, structural and optical characterization of samples

The morphologies of the samples were characterized by scanning electron microscope (SEM, ZEISS Gemini 300) with an accelerating voltage of 3 kV. The structures were determined by X-ray diffraction (XRD, ARL X'TRA) and Raman spectroscopy (Horiba T64000). UV-vis absorption spectra of the samples were obtained using spectroscopy (UV-vis, PE lambda 950). The chemical valence of the samples was investigated by X-ray photoelectron spectroscopy (XPS, PHI5000 Versa Probe) with the calibration of C 1s peak at 284.6 eV.

^{18}O isotope labeling experiments

The ^{18}O isotope labeling experiments were operated in 1 M KOH electrolyte with $H_2{}^{18}O$ as solvent in the dark and under a Xe lamp illumination for 0.5 h. The ^{18}O isotope on the sample surfaces were measured by TOF-SIMS (Münster, Germany) with a negative ion mode, where a beam of Cs^+ ions with the energy of 1 keV sputter onto an area about 300 × 300 μm^2 of samples.

(Photo)electrochemical characterization

The (photo)electrochemical properties of the samples were carried out in a three-electrode by CHI760E electrochemical analyzer under full arc Xe lamp with the intensity of 200 mW/cm^2. The electrolyte was 1 M KOH aqueous solution (pH=13.6). In a three-electrode cell, platinum wire and saturated calomel electrode (SCE) were selected as the counter electrode and the reference electrode, respectively. All of the potentials in this setup were calculated by equation: $E\ (RHE) = E\ (SCE) + 0.059 \times pH + 0.24$. Moreover, the performance of a full device was measured in a two-electrode cell, with the $Fe_2O_3/NiCoO_xH_y$ and Ti-$Fe_2O_3/NiCoO_xH_y$ as photoanodes and the carbon cloth as the counter electrode, respectively.

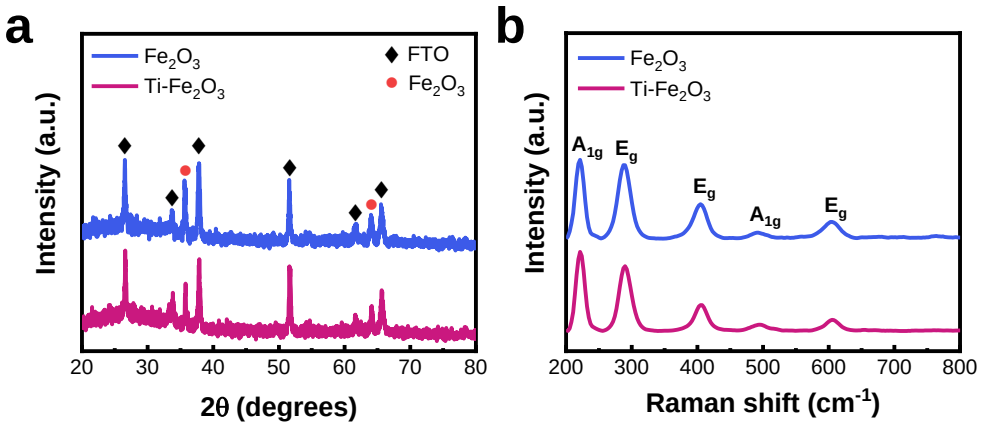

Figure S1. XRD patterns (a) and Raman spectra (b) of Fe_2O_3 and Ti-Fe_2O_3.

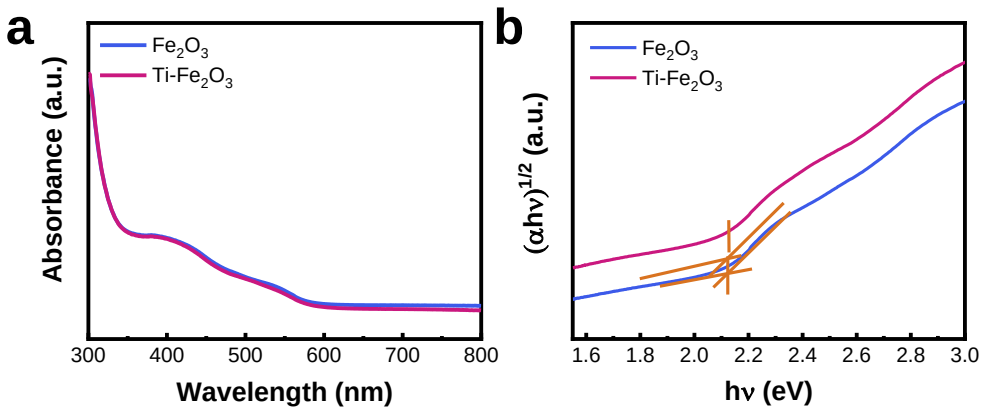

Figure S2. UV-vis adsorption spectra (a) and tauc plots (b) of Fe_2O_3 and Ti-Fe_2O_3.

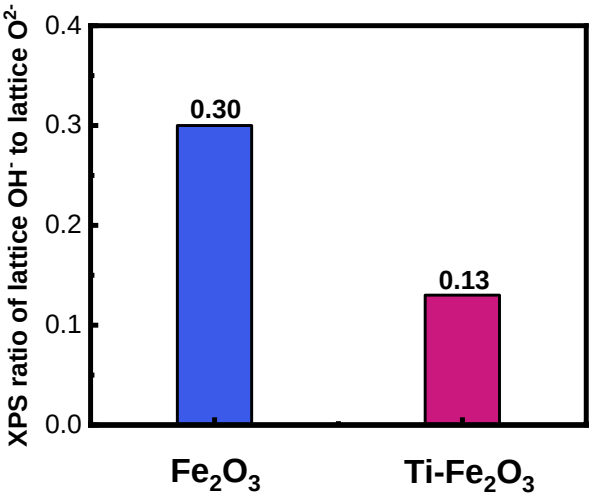

Figure S3. XPS ratio of lattice OH^-/lattice O^{2-} for Fe_2O_3 and Ti-Fe_2O_3.

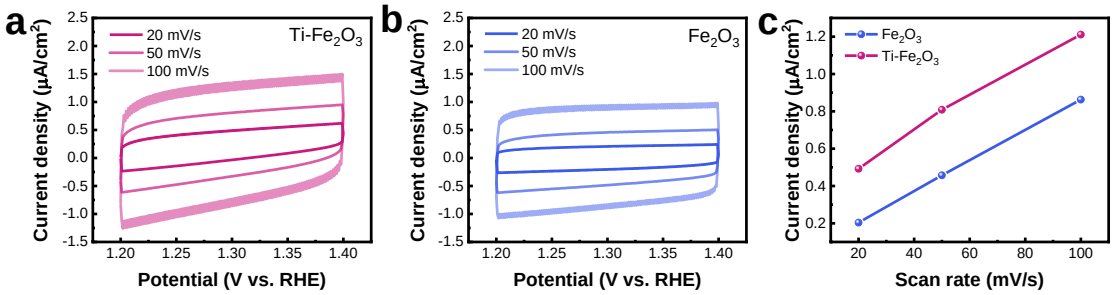

Figure S4. CV curves of Ti-Fe_2O_3 (a) and Fe_2O_3 (b) with different scan rates, electrochemical active surface area of Fe_2O_3 and Ti-Fe_2O_3 calculated from CV curves (c). Electrolyte: 1 M KOH.

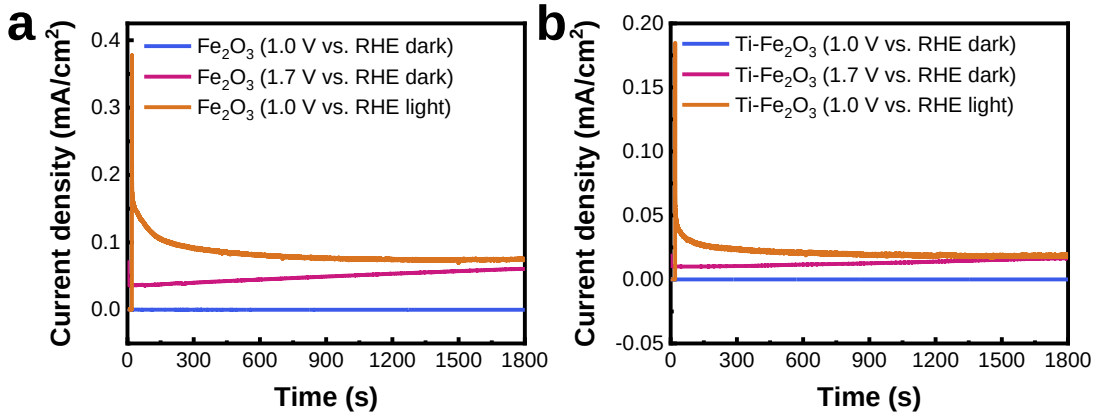

Figure S5. I-T curves of Fe_2O_3 (a) and Ti-Fe_2O_3 (b) oxidized at different conditions. Electrolyte: 1 M KOH($H_2{}^{18}O$).

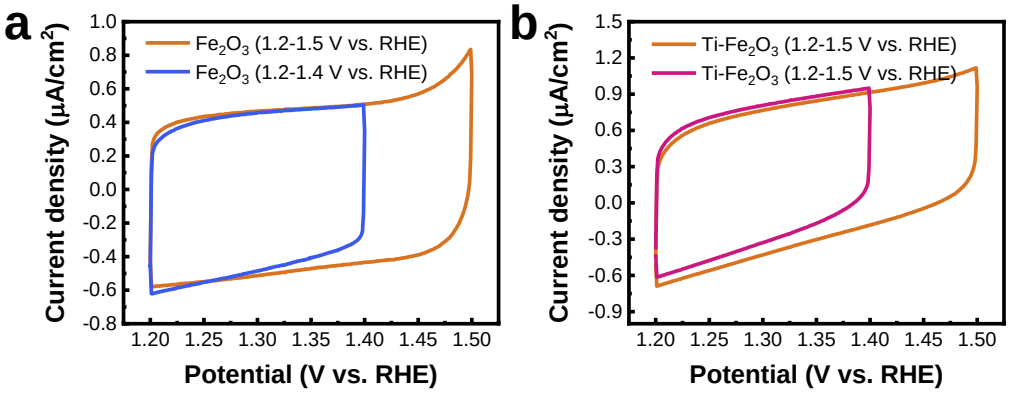

Figure S6. The CV curves of Fe_2O_3 (a) and Ti-Fe_2O_3 (b) in different potential ranges.

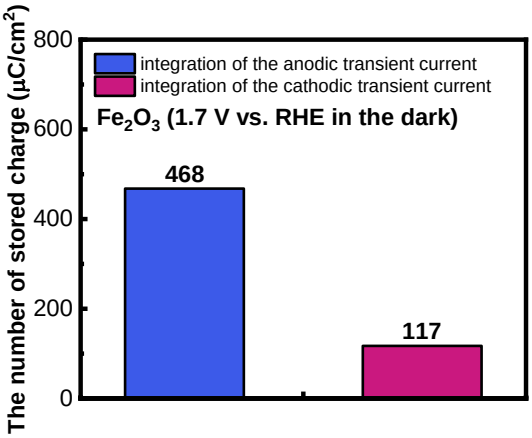

Figure S7. The number of stored charges in the surface faradaic layer of Fe_2O_3 by integrating the anodic transient current and cathodic transient current. E_2: 1.7 V vs. RHE in the dark.

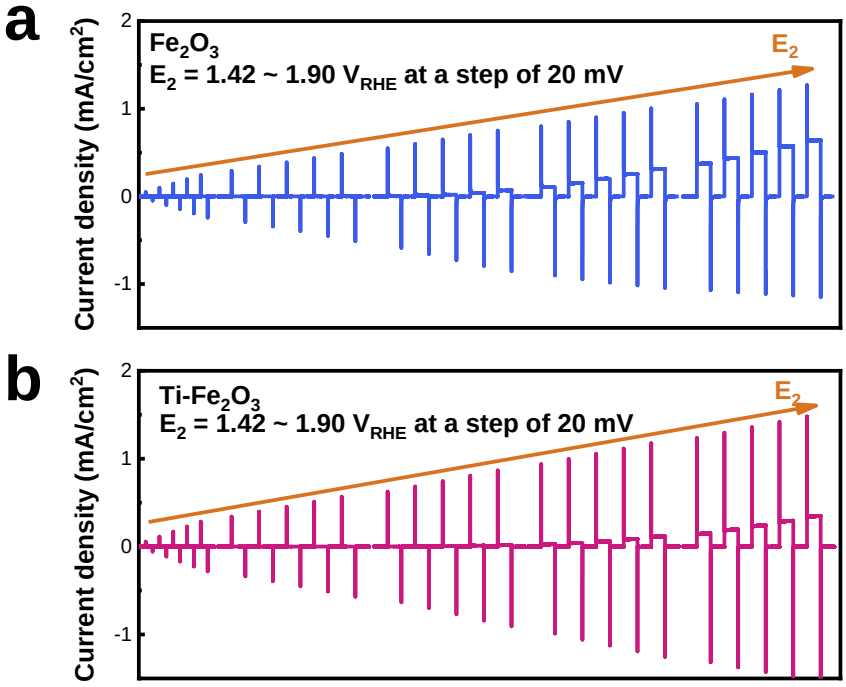

Figure S8. The current responses of Fe_2O_3 (a) and Ti-Fe_2O_3 (b) at different potentials in the dark. The current responses of the two samples were recorded by changing the applied potential of E_2 from 1.42 V vs. RHE to 1.90 V vs. RHE, while E_1 was kept at 1.40 V vs. RHE. The current was monitored with the sample interval of 0.001 s. The DOSC, the number of charge (N) which can be stored in the surface faradaic layer at

different applied potentials (E), is thus calculated by the formula: $\frac{dN}{dE} = \frac{dQ}{edE}$ [3], where the number of stored charges (Q) in the surface faradaic layer was obtained by integrating the cathodic transient current over time by the formula: $Q = \int_0^t idt$.

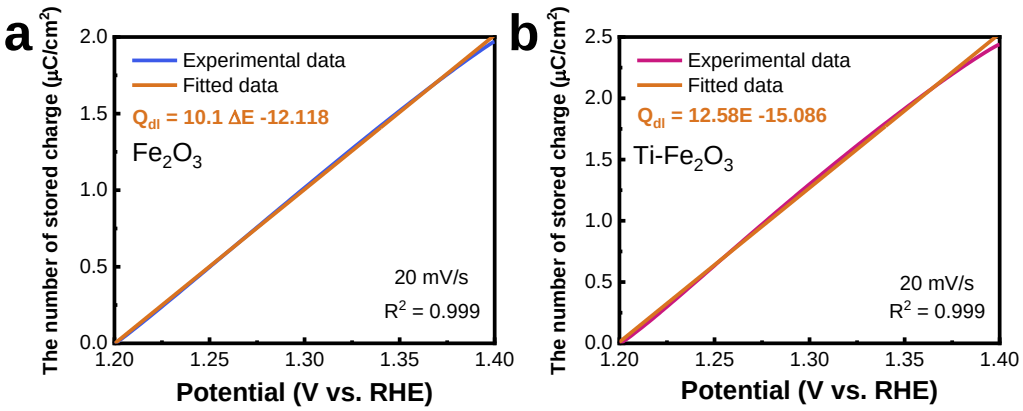

Figure S9. The number of stored charge during double layer charging for Fe_2O_3 (a) and Ti-Fe_2O_3 (b). According to previous work[3], the number of charges during double layer charging can be measured and calculated by CV curves in the potential range of double layer charging (1.2-1.4 V vs. RHE), with the calculation fomula: $\frac{dQ}{dE} = \frac{I_a - I_c}{2\nu}$, where Q is the number of stored charges (C/cm^2), I_a is the anodic current density (A/cm^2), I_c is the cathodic current density (A/cm^2), ν is the scan rate (V/s). As shown in Figure S9, the number of charges during double layer charging for Fe_2O_3 increases linearly with applied potentials, which is consistent with the charging characteristic of double layer. Hence, it can be calculated that the total number of charges during double layer charging in the potential window of surface faradaic layer of Fe_2O_3 (1.4-1.9 V vs. RHE) is about 5 $\mu C/cm^2$. Similarly, the total number of charges during double layer charging for Ti-Fe_2O_3 is about 6.3 $\mu C/cm^2$.

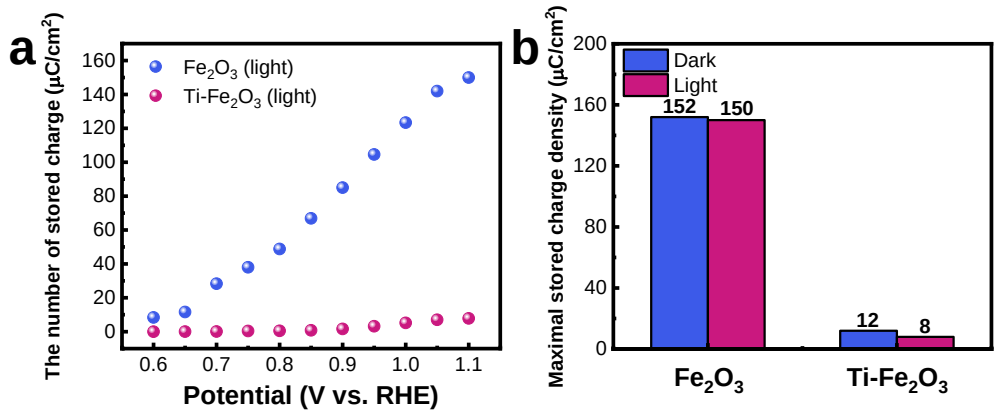

Figure S10. The numbers of stored charges in the surface faradaic layer of Fe_2O_3 and Ti-Fe_2O_3 as a function of applied potentials under illumination (a) and the maximal numbers of stored charges of Fe_2O_3 and Ti-Fe_2O_3 (b) in the dark and under illumination.

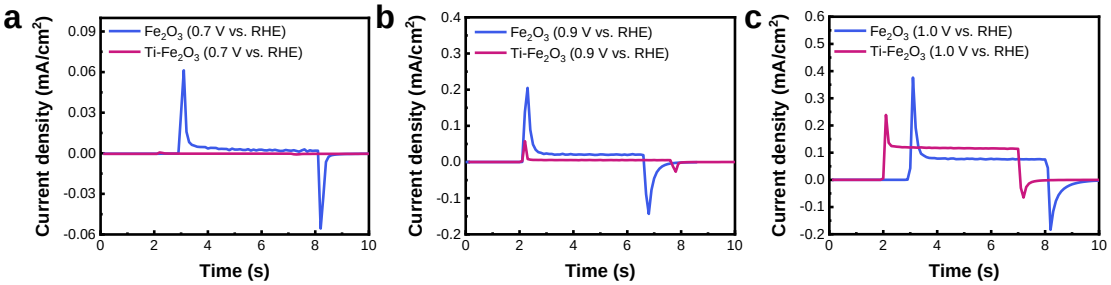

Figure S11. The I-t curves of Fe_2O_3 and Ti-Fe_2O_3 at 0.7 V vs. RHE (a), 0.9 V vs. RHE (b), 1.0 V vs. RHE (c) under chopped light.

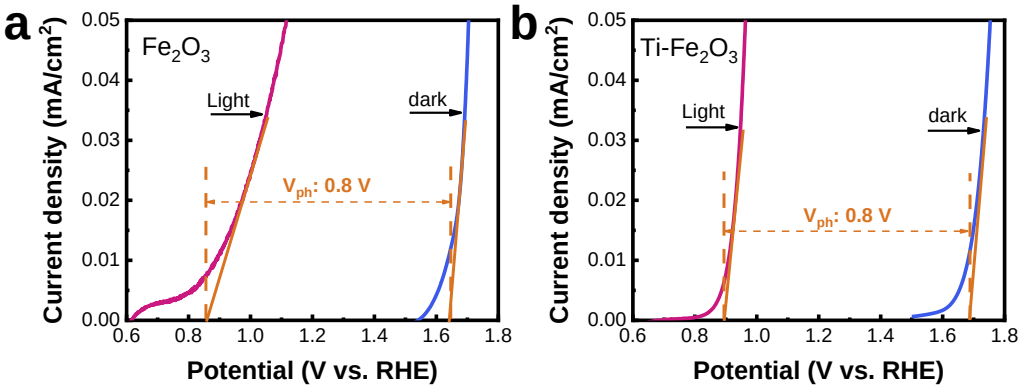

Figure S12. LSV curves of Fe_2O_3 (a) and Ti-Fe_2O_3 (b) in the dark and under illumination. Electrolyte: 1 M KOH, scan rate: 5 mV/s.

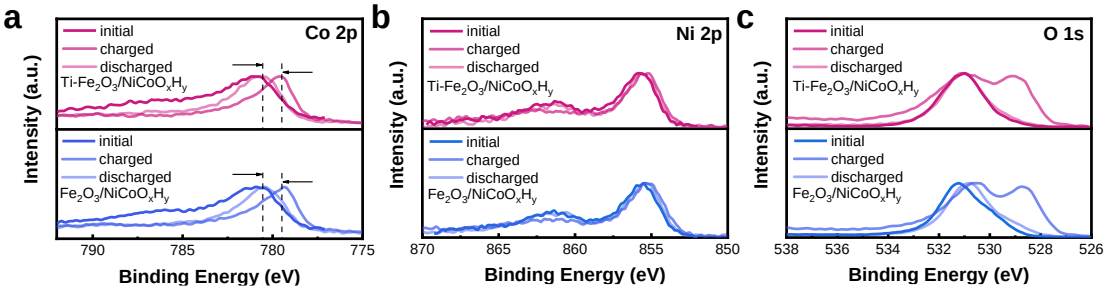

Figure S13. XPS spectra of Co 2p (a), Ni 2p (b) and O 1s (c) in $Fe_2O_3/NiCoO_xH_y$ and Ti-$Fe_2O_3/NiCoO_xH_y$ before and after photocharging and dark discharging.

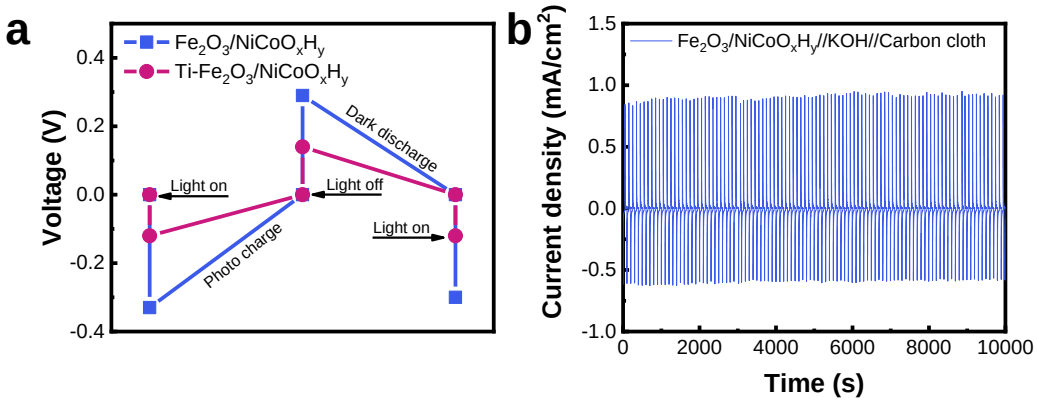

Figure S14. The open circuit voltages of the two solar rechargeable devices (a), cyclic stability of $Fe_2O_3/NiCoO_xH_y$/KOH(aq)/carbon cloth during photo charge and dark discharge (b). Light source: full arc Xe lamp (200 mW/cm^2)

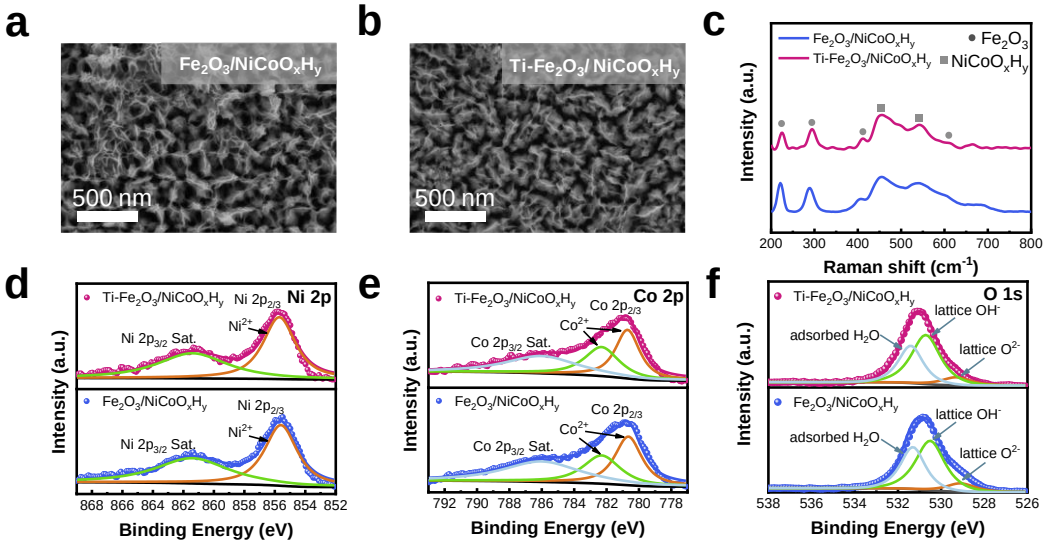

Figure S15. SEM images of $Fe_2O_3/NiCoO_xH_y$ (a) and Ti-$Fe_2O_3/NiCoO_xH_y$ (b), Raman spectra of Ti-$Fe_2O_3/NiCoO_xH_y$, $Fe_2O_3/NiCoO_xH_y$ (c), XPS spectra of Co 2p spectra (d), Ni 2p spectra (e) and O 1s spectra (f) of $Fe_2O_3/NiCoO_xH_y$ and Ti-$Fe_2O_3/NiCoO_xH_y$.

Table S1. The ICP of $Fe_2O_3/NiCoO_xH_y$ and$Ti\text{-}Fe_2O_3/NiCoO_xH_y$

Sample	Ni (μmol)	Co (μmol)
$Ti\text{-}Fe_2O_3/NiCoO_xH_y$	0.06	0.15
$Fe_2O_3/NiCoO_xH_y$	0.07	0.14

References

1. J. W. Jang, C. Du, Y. Ye, Y. Lin, X. Yao, J. Thorne, E. Liu, G. McMahon, J. Zhu, A. Javey, J. Guo and D. Wang, *Nat. Commun.*, 2015, **6**, 7447.
2. M. B. Stevens, L. J. Enman, E. H. Korkus, J. Zaffran, C. D. M. Trang, J. Asbury, M. G. Kast, M. C. Toroker and S. W. Boettcher, *Nano Res.*, 2019, **12**, 2288-2295.
3. P. Wang, M. Xue, D. Jiang, Y. Yang, J. Zhang, H. Dong, G. Sun, Y. Yao, W. Luo and Z. Zou, *Nat. Commun.*, 2022, **13**, 2544.